Chalcogenide Letters Vol. 18, No. 3, March 2021, p. 129 - 135

TITANIUM ALUMINUM CARBIDE COATED D-SHAPED FIBER AS PASSIVE SATURABLE ABSORBER FOR NANOSECOND PULSES GENERATION

A. R. MUHAMMAD[a*], A. A. A. JAFRY[b], A. M. MARKOM[c], S. W. HARUN[d], Z. JUSOH[e], N. KASIM[f], P. YUPAPIN[g,h]

[a]*Institute of Microengineering and Nanoelectronics (IMEN), Universiti Kebangsaan Malaysia (UKM), Bangi, 43600, Selangor, Malaysia*
[b]*Foundation/Diploma, School of Pre-University Studies, Taylor's College Lakeside Campus, No. 1, Jalan Taylor's, 47500 Subang Jaya, Selangor Darul Ehsan.*
[c]*Faculty of Electrical Engineering, Universiti Teknologi MARA (UiTM) Cawangan Johor, Kampus Pasir Gudang, 81750 Johor, Malaysia.*
[d]*Department of Electrical Engineering, University of Malaya, 50603 Kuala Lumpur, Malaysia*
[e]*Faculty of Electrical Engineering, Universiti Teknologi MARA(Terengganu), 23000 Dungun, Terengganu, Malaysia*
[f]*Department of Physics, Faculty of Science, Universiti Teknologi Malaysia, 81310 Skudai, Johor, Malaysia*
[g]*Computational Optics Research Group, Advanced Institute of Materials Science, Ton Duc Thang University, Ho Chi Minh City, Vietnam*
[h]*Faculty of Applied Sciences, Ton Duc Thang University, Ho Chi Minh City, Vietnam*

The saturable absorber device based on the MAX phase titanium aluminum carbide (Ti_3AlC_2) deposited onto D-shaped fiber has successfully activated a pulsed laser at a center wavelength of 1557 nm. The elemental composition and vibrational modes of the saturable absorber were analyzed using energy-dispersive x-ray spectroscopy and Raman spectroscopy for chemical analysis and structure imaging. Strong saturable absorption of 2% and a non-saturable absorption of 49.2% at the 1.55-µm, confirmed its ability to generate pulses in the near-infrared wavelength spectrum. The nanosecond laser owns a pulse width of 146.7 ns, a repetition rate of 3.44 MHz, and a signal-to-noise ratio of 54.4 dB. By varying the laser diode pump from 35-90 mW, a stable short-pulsed laser was generated with the highest single pulse energy of 1.57 nJ, which corresponded to the output power of 5.4 mW. This demonstration shows the potential of MAX phase Ti_3AlC_2 as a saturable absorber in an all fiber-based laser cavity.

(Received December 19, 2020; Accepted March 9, 2021)

Keywords: saturable absorber, erbium-doped fiber laser, Ti_3AlC_2, mode-locking, nanosecond pulses

1. Introduction

It is within the last two decades that avalanche analysis has revealed the nonlinear optical properties for multiple materials and their application in generating short-pulsed laser (SPL)[1]. For instance, Graphene, discovered in 2004 [2], discovered a certain amount of the carbon analogs acted as a material to initiate pulsed laser in a fiber laser cavity [3, 4]. Laser generation in the form of optical pulses was achieved based on the saturable absorption mechanism. Once beam hits the fiber laser cavity and reaches saturable absorber (SA), the photons were captured by the electron within the SA, allowing the electron to leap towards the higher energy state. In the end, every quantum states were filled, and no more electron could transition in between the bands, which obeys the Pauli blocking theory that two or more electrons cannot concurrently occupy the same

* Corresponding author: a.razif@ukm.edu.my
https://doi.org/10.15251/CL.2021.183.129

quantum state. Consequently, the electrons returned to the lower energy state, causing the photons to be released in the form of optical pulses and generating the SPL. This type of laser is essential for numerous industrial and scientific applications, including corrective eye surgery, soft/hard tissue ablation, steel cutting technology, and many others. Therefore, there was a lot of curiosity, all directed at enhancing the efficiency of the lasers, one of the instances is to shorten the laser's pulse duration by choosing a material with outstanding saturable absorption properties [5]. By far, SPL is generated through the application of assorted materials. Generally, the materials can be described into several categories, such as carbon-based materials, transition metal dichalcogenides, topological insulators, metal oxide, metal nanoparticles, organic materials, ternary metal carbides/nitrides (MXene), and several others [6, 7].

As reported in existing studies, perovskite (CH3NH3PbBr3) was found to exert heavy saturable absorption, resulting in substantially stable mode-locking for ytterbium fiber lasers [8, 9]. By utilizing bismuthene nanosheets – microfiber-based 2D materials – as saturable absorber, B. Guo et al. obtained femtosecond range soliton mode-locked EDFL [10]. While other studies managed to obtain substantial optical properties of 2D allotropes, namely few-layer antimonene [11], and titanium disulfide TiS_2[12] which were described functioning in an all-fiber laser cavity as a pulse initiator. Between both of the 2D allotropes, MXene attracts a great deal of interest from scientists and engineers due to its impressive saturable absorption properties. Starting by the study of ultrafast laser generation using MXene $Ti_3C_2T_x$ by Jiang et al. [13], to this date, over 20 publications have been published concerning MXene as a broadband pulse generator [14-17]. MXene is a 2D ternary metal carbide or/and nitride that originates from the MAX phase material. It imitates metal's electronic properties and combined with ceramic's physical characteristics, it is useful for a range of applications. MXene 's ability for ultrafast laser applications has already been exploited; thus, it has also proven useful in the photonics application. Conversely, the works regarding MAX phase, its bulk counterparts, is still limited.

Titanium Aluminum Carbide (Ti_2AlC) is the first material from the MAX phase family. With a 2:1:1 composition, it proves to be an efficient SA in the 1.55-µm region. Lee et al. generate a Q-switched laser with the shortest pulse width of 4.88 µs [18]. In the meantime, various forms of MAX Phase materials, such as V_2AlC [19], Ta_2AlC [20, 21], and Cr_2AlC [22], which have to be discussed, have the potential to exert a distinct output laser behavior based on their distinctive optical properties [23]. At this point, the researchers recently investigated the ability of Ti_3AlC_2 to activate a mode-locked laser in an erbium-doped fiber laser (EDFL) cavity [24], trailed with the successful generation of 1-µm Q-switched laser from the same material [25]. By analyzing Ti_3AlC_2's optical properties, the study determined the adequate saturable absorption of the thin film of Ti_3AlC_2 with a 2% modulation depth resulting from the linear absorption of 3 dB. However, with this thin-film structure, the laser's reliability at a high pump intensity cannot be maintained. It was found that the thin-film with different polymer as a host suffers from a photo-darkening effect, resulting the mechanical and physical breakdown to the SA device, and it burns the tip of fiber-ferrule. In this regard, this problem has been solved by implementing different SA in a fiber laser cavity. The development of the SA device with Ti_3AlC_2 MAX phase deposited onto the D-shaped fiber (MAX-DSF) was demonstrated. The obtained MAX-DSF SA possess a saturable absorption of 2%, the non-saturable absorption of 49.2%, with capacity to generate a nanosecond pulsed laser with a pulse width of 146.7 ns. The laser operates steadily within the pump power of 35 to 90 mW at the operating wavelength of 1557 nm. As far as the researchers' knowledge, this is the first demonstration of SPL with a MAX phase deposited onto the D-shaped fiber in an all fiber-based laser cavity.

2. Preparation, characterization, and nonlinear absorption spectrum of Ti_3AlC_2

The SA device was synthesized based on the liquid casting process, providing a convenient preparation process compared to most other techniques [26, 27]. The key components were polyvinyl alcohol (PVA), deionized (DI) water, and the Ti_3AlC_2 powder. They undergo mixing process and were ultrasonicated to obtain the liquid SA mixture. First, the PVA solution

was synthesized by mixing 1 g of its powder with 120 mL of DI water under the temperature of 200 °C with a stirring speed of 300 rpm. Next, the solution was mixed with the Ti_3AlC_2 powder by stirring process and ultrasonication. With 10 mg of the powder and 40 mL of PVA solution, they were stirred for 24 hrs, followed by the ultrasonication for 2 hrs. The effectiveness of the procedure was proven by a gritty particle appearance at the bottom of the beaker. Only the supernatant was used as a SA and deposited onto the D-shaped fiber. A 3 µL solution was used as a SA, dropped on the D-shaped fiber with the EDFL cavity operates in the CW regime. Finally, the MAX-DSF SA was left to dry for 3 hrs at room temperature.

Validation on the SA's characteristics were made through the energy-dispersive x-ray spectroscopy (EDS), Raman spectroscopy, and variable-pressure scanning electron microscopy (VP-SEM). As shown in Fig. 1 (a), the EDS spectrum showed four primary composite elements of Ti_3AlC_2. Titanium, as the main element, owns a 73.2% weight, while only 10.5% weight of aluminum is traced from the measurement. The carbon and oxygen represent 9.3% and 7% of the total elemental compositions. Further verification on the vibrational modes was determined by using UniDRON, Confocal microscope Raman spectroscopy. It unveils the spectrum in Fig. 1 (b) with six Raman peaks, parallel to the theoretical prediction by Presser et al. [28]. The first four peaks illustrate the active phonon vibration modes of Ti_3AlC_2, and the final peak of the spectrum represent the disordered carbon in the composition. The peak at the wavenumber of 171 cm^{-1}, 407 cm^{-1}, 517 cm^{-1}, and 638 cm^{-1} was assigned to the Raman modes of E_g, E_{2g}, E_{1g}, and A_{1g}. The last two peaks located at the 1318 cm^{-1} and 1281 cm^{-1} represents the D and G bands of disordered carbon. Those two measurements verify the presence of Ti_3AlC_2 in the developed SA. Finally, the balanced-twin detector technique unveils the nonlinear absorption spectrum of the MAX-DSF. As illustrated in Fig. 1 (c), the SA owns a saturable absorption of 2%, a non-saturable absorption of 49.2%, and a saturable intensity (I_{sat}) of 2.68 MW/cm^2. Those values were comparable to its thin-film equivalents, which unveils a modulation depth of 2% with a non-saturable absorption of 58.2% [24]. A stable 3.6 ps mode-locked at the 1558 nm was used as the laser source for the measurement. Thus, the developed SA device could generate pulsed laser in the 1.55-µm region.

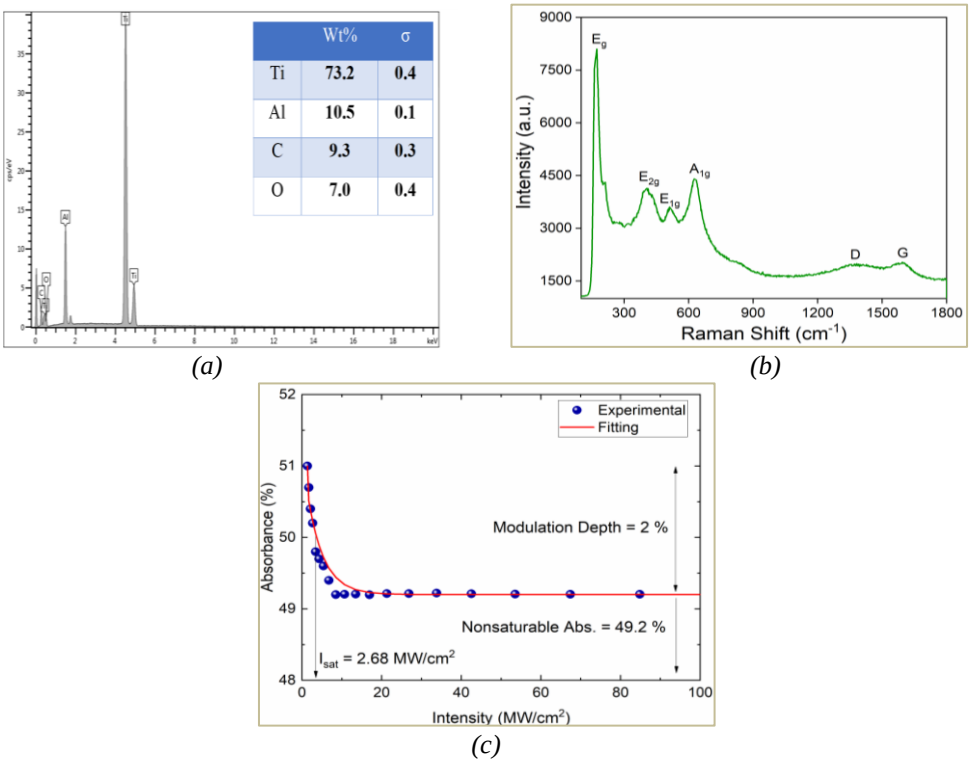

Fig. 1. Characterization of Ti_3AlC_2; (a) EDS spectrum, (b) Raman spectrum, (c) nonlinear absorption profile at 1.55-µm region.

3. Experimental configuration for a nanosecond pulsed generation in an EDFL cavity

The EDFL cavity combined with the optical components was designed to explore the ability of MAX-DSF as an SA device. As illustrated in Fig. 2 (a), the 980 nm laser diode (LD) emission was exploited to obtain an excitation of energy in the laser configuration. The light passed through the wavelength division multiplexer (WDM) with two input ports, and one of the ports was directly spliced to the LD. The light then travelled towards an erbium-doped fiber (EDF) to trigger the stimulated emission working under the 1.55-µm regime. The EDF has a length of 2.4 m, a coefficient of absorption at 23.9 dB/m, a numerical aperture of 0.24, and a core/cladding diameter of 9/125 µm. The light was forced to disseminate in one direction via optical coupler which then spliced to a 50 m single-mode fiber (SMF-28) to optimize the length of cavity and regulate the dispersion and nonlinearity, encouraging the SPL generation. The flowing light in the cavity then reaches the MAX-DSF, which stabilized the ultrashort pulse. An optical coupler, with 20% extracted from the cavity were directed to measuring instruments for analysis purposes, while the other 80% continues circulating inside the laser configuration. The measuring instruments used were the digital oscilloscope (GWINSTEK, GDS3352), optical spectrum analyzer (ANRITSU, MS9710C), radio frequency spectrum analyzer (7.8 GHz ANRITSU, MS2683A), and optical power meter. The oscilloscope and radio frequency spectrum analyzer were linked to the cavity via an InGaAs photodetector. In total, the length of cavity accounts for 64.4 m. It demonstrates a group density dispersion of -1,416 ps2, suggesting that the ML EDFL resides under the anomalous dispersal regime. The individual components own a group velocity dispersion of -21.7 ps^2/km (SMF-28) and -27.6 ps^2/km (EDF). The laser configuration as constructed generates a continuous-wave (CW) laser at the pump power of 16 mW. The generation of the CW regime was verified by the captured OSA spectrum with a central wavelength of 1560 nm, as shown in Fig. 2 (b). Next, the MAX-DSF SA triggered an SPL generation at the threshold pump power of 35 mW. The stable ML laser was retained without visible pulse disruption by tuning the input power from 35 to 90 mW.

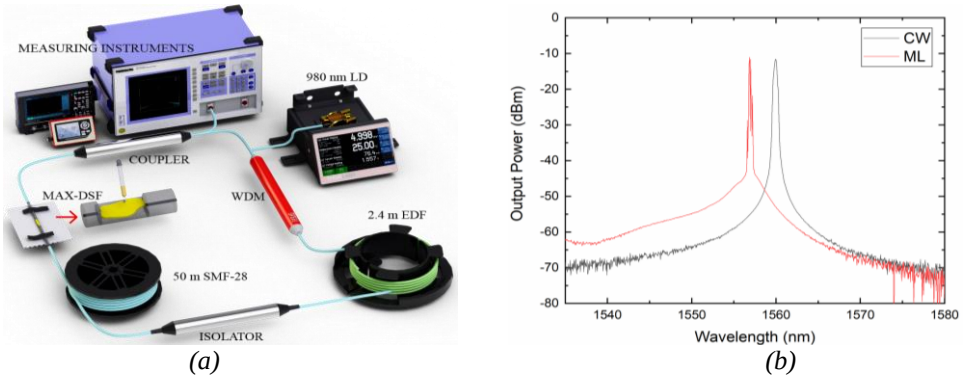

Fig. 2. (a) Experimental configuration for nanosecond pulse generation in an EDFL cavity with a Ti_3AlC_2 deposited onto D-shaped fiber as SA. (b) generated optical spectrum at continuous wave and mode-locked operation.

4. The generation of nanosecond pulsed with Ti_3AlC_2 deposited onto D-shaped fiber

Fig. 3 (a) illustrates the oscilloscope trace of ML at the moderate input power of 67 mW. Slight amplitude fluctuation of the sinusoidal waves resulted from the timing jitter's presence, due to the low intracavity pulse energy in the laser configuration [29]. The close-ups image of the two adjacent pulses within a 600 ns period was depicted in Fig. 3 (b). Based on the observation, the two waveforms reflect a crest-to-crest distance of 290.4 ns while the full-width half-maximum (FWHM) measured for a single pulse was 146.7 ns. An RF spectrum was captured within a 50

MHz frequency to validate the stability of the generated ML, as shown in Fig. 3 (c). The frequency obtained at the first peak was 3.44 MHz. This value corresponds to the pulse duration reported at the trace of the oscilloscope which was 290.4 ns. The signal-to-noise ratio (SNR) of ~54.4 dB indicates an ML laser with a low resonant relaxation oscillation frequency [30]. The cavity length of 64.4 m is aligned with the repeat rate of 3.44 MHz, which corresponds to the cavity's average round trip time (290.4 ns).

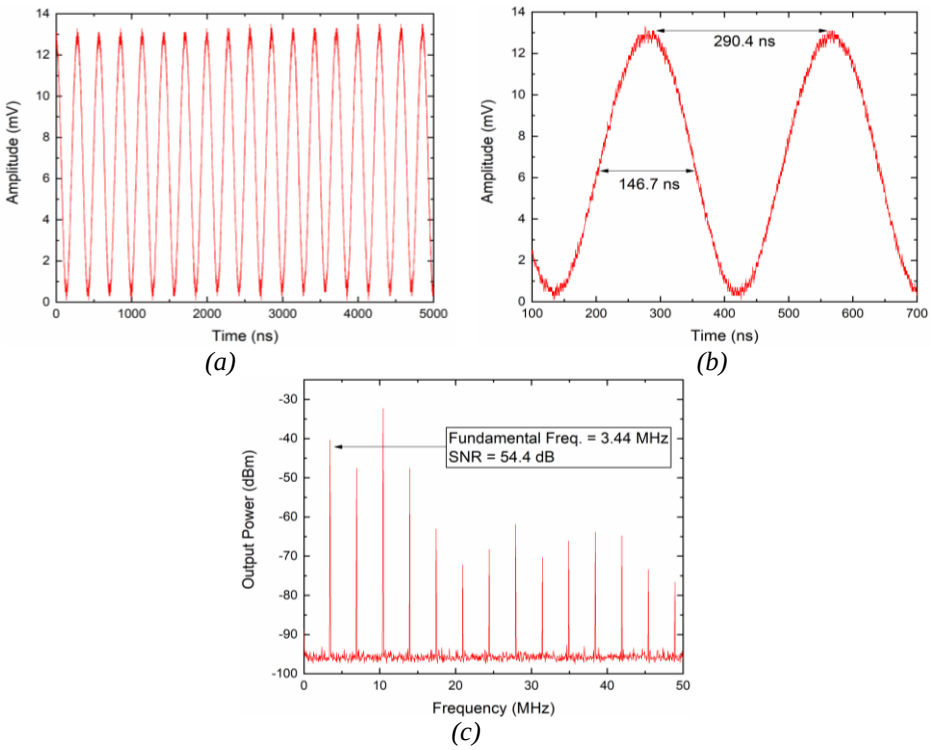

Fig. 3. Temporal performances of the generated SPL; (a) oscilloscope spectrum, (b) two pulses envelopes, and (c) radio frequency spectrum.

The temporal output reported from the oscilloscope was traced in Fig. 4 (a). An almost uniform repeat rate within the input range of 35 to 90 mW suggested a reliable ML laser operation. The laser generated the repetition rate with a standard deviation of 0.00105 MHz, calculated between the value of 3.442-3.445 MHz. The pump power varies between 35-90 mW generates the pulse width of 144.8-148 ns with a standard deviation of 0.8607 ns, implying a consistent pulsed laser. The output properties of the produced pulsed laser were measured by using an optical power meter. This measurement yields a graph in Fig. 4 (b). The graph illustrates the output power obtained as the pump power adjusted from 35 to 90 mW, with the maximum value obtained was 5.4 mW. Through the gradient projected, the slope efficiency is calculated containing a high-power conversion efficiency of 7%. Concurrently, the pulse energy and peak power recorded were linearly increased with the increase in pump power, as illustrated in Fig. 4 (b), resulting in the maximum attainable pump power of ML (90 mW) corresponding with the highest pulse energy of 1.57 nJ and peak power of 10.7 mW. The significant output properties indicate a low loss laser cavity and the SA device with excellent nonlinear absorption properties.

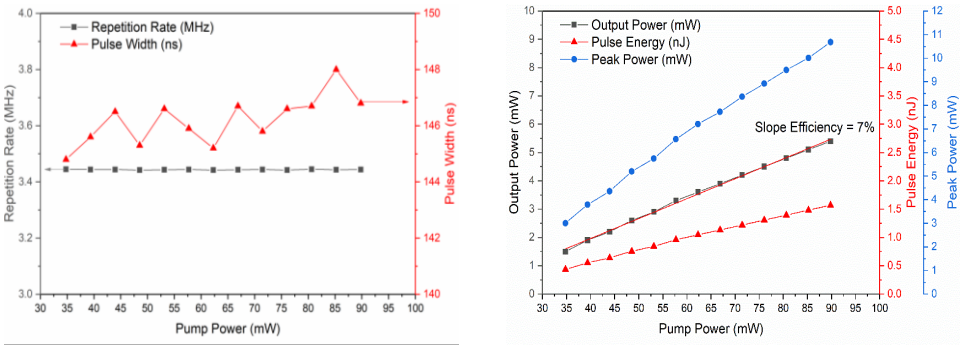

(a) *(b)*

Fig. 4. SPL performances with the variation of pump power; (a) The graph of repetition rate and pulse width as a function of pump power, and (b) the graph of output power, pulse energy, and peak power as a function of pump power.

5. Conclusion

To sum up, the research shows the MAX stage Ti_3AlC_2 potential as a saturable absorber in the 1.55-µm regime. The evanescent field activity on the surface of the D-formed film was demonstrated successfully by several drops of Ti_3AlC_2. A reliable nanosecond pulse laser has also been produced by integrating the SA device into the EDFL cavity. This laser generates an output revolving around 1557 nm as the pump power is set from 35 to 90 mW. The pulse width and repetition rate recorded was 146.7 ns and 3.44 MHz at the moderate input power of 67 mW. The results also suggest an alternative, which is to adopt the thin-film SA device since the produced MAX-DSF has a 2 % modulation depth comparable to its thin-film counterparts. The first analysis on the D-shaped fiber coated with the MAX phase-based SA founding a new pathway towards versatile SA in an all-fiber based cavity.

Acknowledgements

The authors would also like to thank the Ton Duc Thang University, Vietnam, Department of Physics, Universiti Teknologi Malaysia, and Photonics Engineering Laboratory, University of Malaya, for the research facility provided throughout this work.

References

[1] S. Li, C. Wang, Y. Yin, E. Lewis, P. Wang, Novel layered 2D materials for ultrafast photonics, (0) 20200030 (2020).
[2] K. S. Novoselov, A. K. Geim, S. V. Morozov, D. Jiang, Y. Zhang, S. V. Dubonos, I. V. Grigorieva, A. A. Firsov, Science **306**(5696), 666 (2004).
[3] Q. L. Bao, H. Zhang, Y. Wang, Z. H. Ni, Y. L. Yan, Z. X. Shen, K. P. Loh, D. Y. Tang, Advanced Functional Materials **19**(19), 3077 (2009).
[4] M. Chernysheva, C. Mou, R. Arif, M. AlAraimi, M. Rümmeli, S. Turitsyn, A. Rozhin, Scientific Reports **6**, 24220 (2016).
[5] D. Li, H. Jussila, L. Karvonen, G. Ye, H. Lipsanen, X. Chen, Z. Sun, Sci. Rep. **5**, 15899 (2015).
[6] B. H. Chen, X. Y. Zhang, K. Wu, H. Wang, J. Wang, J. P. Chen, Optics Express **23**(20), 26723 (2015).
[7] L. N. Duan, Y. G. Wang, C. W. Xu, L. Li, Y. S. Wang, IEEE Photonics J. **7**(2), 7 (2015).
[8] P. Li, Y. Chen, T. Yang, Z. Wang, H. Lin, Y. Xu, L. Li, H. Mu, B. N. Shivananju, Y. Zhang, Q. Zhang, A. Pan, S. Li, D. Tang, B. Jia, H. Zhang, Q. Bao, ACS Appl Mater Interfaces

9(14), 12759 (2017).
[9] Y. Zhang, C.-K. Lim, Z. Dai, G. Yu, J.W. Haus, H. Zhang, P. N. Prasad, Physics Reports **795**, 1 (2019).
[10] B. Guo, S. H. Wang, Z. X. Wu, Z. X. Wang, D. H. Wang, H. Huang, F. Zhang, Y. Q. Ge, H. Zhang, Opt. Express **26**(18), 22750 (2018).
[11] Y. Song, Z. Liang, X. Jiang, Y. Chen, Z. Li, L. Lu, Y. Ge, K. Wang, J. Zheng, S. Lu, J. Ji, H. Zhang, 2D Materials **4**(4), (2017).
[12] Y. Ge, Z. Zhu, Y. Xu, Y. Chen, S. Chen, Z. Liang, Y. Song, Y. Zou, H. Zeng, S. Xu, H. Zhang, D. Fan, Advanced Optical Materials **6**(4), (2018).
[13] X. T. Jiang, S. X. Liu, W. Y. Liang, S. J. Luo, Z. L. He, Y. Q. Ge, H. D. Wang, R. Cao, F. Zhang, Q. Wen, J. Q. Li, Q. L. Bao, D. Y. Fan, H. Zhang, Laser Photon. Rev. **12**(2), 10 (2018).
[14] J. J. Feng, X. H. Li, T. C. Feng, Y. M. Wang, J. Liu, H. Zhang, Annalen Der Physik **532**(1), 7 (2020).
[15] Y. I. Jhon, J. Koo, B. Anasori, M. Seo, J. H. Lee, Y. Gogotsi, Y. M. Jhon, Adv. Mater. **29**(40), 1702496 (2017).
[16] W. Huang, C. Ma, C. Li, Y. Zhang, L. Hu, T. Chen, Y. Tang, J. Ju, Nanophotonics 9 (2020).
[17] A. A. A. Jafry, G. Krishnan, N. Kasim, N. F. Zulkipli, F. S. M. Samsamnun, R. Apsari, S. W. Harun, Opt. Fiber Technol. **58**, 102289 (2020).
[18] J. Lee, S. Kwon, J. H. Lee, Optical Materials Express **9**(5), 2057 (2019).
[19] Z. Sun, R. Ahuja, S. Li, J. M. Schneider, Applied Physics Letters **83**(5), 899 (2003).
[20] C. Hu, L. He, J. Zhang, Y. Bao, J. Wang, M. Li, Y. Zhou, Journal of the European Ceramic Society **28**(8), (2008) 1679.
[21] J. Etzkorn, M. Ade, H. Hillebrecht, Inorg. Chem. **46**(4), 1410 (2007).
[22] B. Manoun, R. P. Gulve, S. K. Saxena, S. Gupta, M. W. Barsoum, C. S. Zha, Physical Review B **73**(2), (2006).
[23] Y. Mo, P. Rulis, W. Y. Ching, Physical Review B **86**(16), (2012).
[24] A. A. A. Jafry, N. Kasim, M. F. M. Rusdi, A. H. A. Rosol, R. A. M. Yusoff, A. R. Muhammad, B. Nizamani, S. W. Harun, Optics & Laser Technology **127**, 106186 (2020).
[25] A. R. Muhammad, A. A. A. Jafry, A. M. Markom, A. H. A. Rosol, S. W. Harun, P. Yupapin, Appl. Optics **59**(18), 5408 (2020).
[26] X. Jiang, W. Li, T. Hai, R. Yue, Z. Chen, C. Lao, Y. Ge, G. Xie, Q. Wen, H. J. N. D. M. Zhang, Applications, Inkjet-printed MXene micro-scale devices for integrated broadband ultrafast photonics, **3**(1), 1 (2019).
[27] M. Q. Lokman, S. Yusoff, F. Ahmad, R. Zakaria, H. Yahaya, S. Shafie, R. M. Rosnan, S. W. Harun, Results Phys. **11**, 232 (2018).
[28] V. Presser, M. Naguib, L. Chaput, A. Togo, G. Hug, M. W. Barsoum, First-order Raman scattering of the MAX phases: Ti2AlN, Ti2AlC0.5N0.5, Ti2AlC, (Ti0.5V0.5)2AlC, V2AlC, Ti_3AlC_2, and Ti3GeC2, **43**(1), 168 (2012).
[29] R. Paschotta, Optics Express **18**(5), 5041 (2010).
[30] W. Yue, Y. Wang, C.-D. Xiong, Z.Y. Wang, Q. Qiu, J. Opt. Soc. Am. B **30**(2), 275 (2013).